

# Delay differential equations for mode-locked semiconductor lasers

Andrei G. Vladimirov\*

Weierstrass Institute for Applied Analysis and Stochastics, Mohrenstrasse 39, D-10117 Berlin, Germany

Dmitry Turaev

Ben Gurion University, P.O. Box 653, 84105 Beer-Sheva, Israel

Gregory Kozyreff

Oxford Center for Industrial and Applied Mathematics, Oxford University, Oxford OX1 3LB, UK

Received February 9, 2004

We propose a new model for passive mode locking that is a set of ordinary delay differential equations. We assume a ring-cavity geometry and Lorentzian spectral filtering of the pulses but do not use small gain and loss and weak saturation approximations. By means of a continuation method, we study mode-locking solutions and their stability. We find that stable mode locking can exist even when the nonlasing state between pulses becomes unstable. © 2004 Optical Society of America

OCIS codes: 140.4050, 140.5960, 190.3100.

Passive mode locking (ML) of lasers is a very effective technique to generate high-quality short pulses with high repetition rates. Monolithic semiconductor lasers, passively or hybrid mode locked, are ideal for applications in high-speed telecommunications on account of their compactness, low cost, and reliability.<sup>1</sup> The basic mechanism for passive ML is well understood since the analysis by New,<sup>2</sup> who showed that the differential saturation of the gain and losses in the laser cavity opens a short temporal window of net gain for pulses. A wide range of experimental, numerical, and analytical methods exist to characterize ML (for an overview, see Haus<sup>3</sup> and Avrutin *et al.*<sup>4</sup>). Although numerical integrations of traveling-wave field equations coupled to material equations (distributed models) faithfully reproduce experimental observations, they offer little insight into the underlying dynamics. This is why analytical approaches based on lumped element models, mainly those introduced by New<sup>2</sup> and Haus and co-workers<sup>3,5–8</sup> are still widely used. Inevitably, though, these approaches require certain approximations that in many cases are hardly satisfied experimentally. New, for instance, assumed small gain and loss per cavity round trip and ignored spectral filtering. Haus did take spectral filtering into consideration under the parabolic approximation and showed how even an infinite bandwidth alters ML stability.<sup>5</sup> Further approximations, such as the assumption of weak saturation, had to be made during the process. Yet the agreement between analytical results and experimental data on the dye laser<sup>7</sup> motivated many studies of variations of Haus's model.<sup>4</sup>

In this Letter we propose and discuss a new model for passive ML that is a set of ordinary delay differential equations (DDEs). In doing so we avoid the approximations of small gain and loss per cavity round trip and weak saturation; these do not hold well in

semiconductor laser devices. On the other hand, as in most lumped element models, we neglect the spatial effects, such as spatial hole burning and self-interference of the pulse near the mirrors, inherent in a linear cavity. This amounts to considering a unidirectional lasing ring cavity. Absorbing, amplifying, and spectral filtering segments are placed in succession in the cavity. Let  $a(t)$  be the field amplitude at the entrance of the absorber section [defined such that  $|a(t)|^2$  is the optical power]. The relations among the input and output fields in these segments are given by  $a_1(t) = \exp[-(1 - i\alpha_q)q(t)/2]a(t)$ ,  $a_2(t) = \exp[(1 - i\alpha_g)g(t)/2]a_1(t)$ , and  $a_3(t) = \int_{-\infty}^t f(t - \theta)a_2(\theta)d\theta$ .<sup>4,5</sup> In these relations  $g(t)$  and  $q(t)$  are saturable gain and losses, respectively, and  $\alpha_{g,q}$  are the linewidth-enhancement (self-phase modulation) factors. The cavity and semiconductor material dispersive effects are taken into account by the linear impulse response function  $f(t)$ . Finally, given cavity round-trip time  $T$ ,  $a(t + T) = \sqrt{\kappa}a_3(t)$ , where  $\sqrt{\kappa} < 1$  is the linear non-resonant attenuation factor per pass. Substituting these relations into one another, we obtain

$$a(t + T) = \sqrt{\kappa} \int_{-\infty}^t f(t - \theta) \exp[(1 - i\alpha_g)g(\theta)/2 - (1 - i\alpha_q)q(\theta)/2] a(\theta) d\theta. \quad (1)$$

Then, using the procedure described in Ref. 9, we obtain the equations for  $g(t)$  and  $q(t)$ :

$$\dot{g}(t) = g_0 - \gamma_g g(t) - \exp[-q(t)] \{ \exp[g(t)] - 1 \} |a(t)|^2 / E_g, \quad (2)$$

$$\dot{q}(t) = q_0 - \gamma_q q(t) - \{ 1 - \exp[-q(t)] \} |a(t)|^2 / E_q. \quad (3)$$

Here,  $g_0$  and  $q_0$  stand for unsaturated gain and absorption, respectively, and  $\gamma_r$  and  $E_r$  ( $r = g, q$ ) are the

carrier density relaxation rate and the saturation energy in the gain and absorbing sections, respectively. Especially important in the laser dynamics is the ratio  $s = E_g/E_q$ .

Typical monolithic devices comprise Bragg reflectors, whose frequency bandwidth is much narrower than that of the material gain. Hence, the spectral filtering of the cavity is determined mainly by the mirrors. We assume it to be Lorentzian, i.e.,  $f(t) = \gamma \exp(-\gamma t)$ . This is valid when close enough to the main peak of the spectral reflectance and if the Bragg response is reactive only.<sup>10</sup> Equation (1) can then be replaced with the DDE:

$$\begin{aligned} \gamma^{-1}\dot{a}(t) + a(t) = & \sqrt{\kappa} \exp[(1 - i\alpha_g)g(t - T)/2 \\ & - (1 - i\alpha_q)q(t - T)/2]a(t - T). \end{aligned} \quad (4)$$

Indeed, the general solution of Eq. (4) is given by  $a(t) = a(0)\exp(-\gamma t) + \int_0^t \exp[\gamma(\theta - t)]\text{rhs}(\theta - T)d\theta$ , where  $\text{rhs}(t - T)$  is the right-hand side of Eq. (4), and it coincides with Eq. (1), provided that  $a(0) = \int_{-\infty}^0 \exp(\gamma\theta)\text{rhs}(\theta - T)d\theta$ . Strictly speaking, Eq. (4) is equivalent to Eq. (1) only under this specific initial condition. However, since in the long time limit the effect of the initial condition on the solution decays exponentially in time, its precise form can be safely ignored.

Equations (2)–(4) constitute the new model of this Letter. New's results<sup>2</sup> can be obtained by setting  $\gamma^{-1}\dot{a}(t) = 0$  in Eq. (4) and expanding all exponentials up to the first-order terms in  $g$  and  $q$ . If, on the other hand, one neglects the relaxation terms in Eqs. (2) and (3), substitutes their solutions into Eq. (4), expands to second order in pulse energy, and finally assumes periodicity with period  $T + \delta T$ , then, using  $a(t) \approx a(t - T) + \delta T\dot{a}(t - T)$  on the left-hand side of Eq. (4), we can recover Haus's sech solution.

One advantage of this new formulation of the ML problem is that it allows us to make use of techniques that have been developed for DDE systems. From now on, for simplicity, we restrict our numerical analysis to the case in which  $\alpha_{g,q} = 0$  in Eq. (4).

The constant-intensity (cw) solution of Eqs. (2)–(4) exists above the linear threshold,  $g_0/\gamma_g > q_0/\gamma_q - \ln \kappa$ . Its bifurcation diagram is shown in Fig. 1 in the  $(g_0, q_0)$  plane for the parameter values given in the figure caption. Curves  $H_n$  indicate Andronov–Hopf bifurcation to time-periodic intensity with period close to  $T/n$ . Thus curve  $H_1$  corresponds to the fundamental ML regime with pulse repetition frequency close to  $\Omega_1 = 2\pi/T$ , and curves  $H_n$  with  $n = 2, 3, 4$  signal the onset of multiple-pulse ML regimes with repetition frequencies close to  $n\Omega_1$ . On the other hand,  $H_Q$  is an Andronov–Hopf bifurcation with a frequency approximately eight times smaller than  $\Omega_1$ . This bifurcation is responsible for the  $Q$ -switching instability.

Similarly to the Andronov–Hopf bifurcation curves the branches of periodic solutions and their stability have been calculated numerically with DDE-BIFTOOL.<sup>11</sup> The result is shown in Fig. 2 for  $q_0 = 2\gamma_q$ . One can see from the figure that branch

$P_1$ , corresponding to the fundamental ML regime, has two stability ranges. The first is very narrow and located near the left-hand Andronov–Hopf bifurcation point at small values of  $g_0$ , where the amplitude of  $P_1$  is small. Therefore the probability of observing the ML regime in this range experimentally seems to be very low. The second stability range is limited by two bifurcation points. The left-hand one is a secondary Andronov–Hopf bifurcation point labeled QP. This bifurcation produces a solution with quasi-periodic laser intensity that corresponds to a ML regime modulated by the  $Q$ -switching frequency. With a decrease of pump parameter  $g_0$  below the QP point, the modulation depth grows. This is in agreement with the experimental results of Ref. 12, where a gradual transition from a ML regime to a self-pulsing one was observed with a decrease of the gain current. Another bifurcation point, SN, is a saddle-node bifurcation whereby two periodic intensity solutions, one stable and another unstable, merge and disappear. The solutions corresponding to multiple-pulse ML are labeled  $P_2$  and  $P_3$  in Fig. 2. These solutions undergo bifurcations similar to those of the fundamental

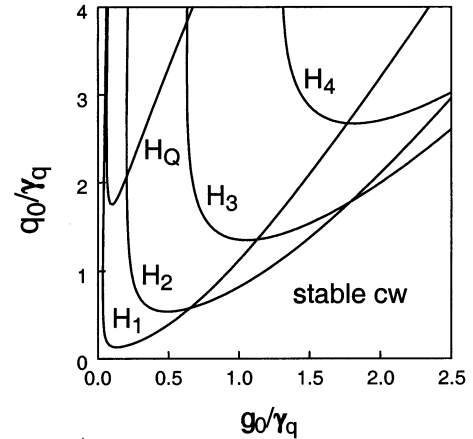


Fig. 1. Andronov–Hopf bifurcations of the cw solution of Eqs. (2)–(4). The parameters are  $T = 25$  ps,  $\gamma^{-1} = 0.4$  ps,  $\alpha_{g,q} = 0$ ,  $s = 5$ ,  $\gamma_g^{-1} = 1$  ns,  $\gamma_q^{-1} = 10$  ps, and  $\kappa = 0.5$ .

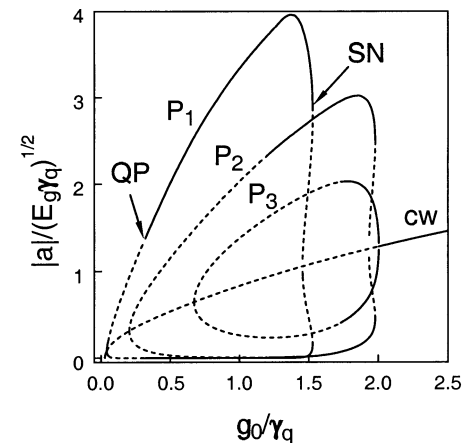


Fig. 2. Branches of ML solutions bifurcating from the Andronov–Hopf bifurcation curves shown in Fig. 1. The solid (dashed) curves indicate stable (unstable) solutions. The branch of constant-intensity solutions is labeled cw.  $q_0 = 2\gamma_q$ . The other parameters are the same as in Fig. 1.

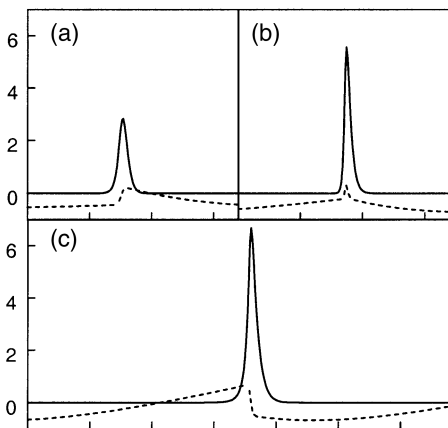


Fig. 3. Time dependence of the amplitude (solid curves) of a fundamental ML pulse and the net gain parameter (dashed curves). (a)  $g_0 = 0.4\gamma q$ , (b)  $g_0 = 0.8\gamma q$ , (c)  $g_0 = 1.32\gamma q$ . The other parameters are the same as in Fig. 2.

branch  $P_1$ . From Fig. 2 one can notice that bistability exists between different ML regimes for some ranges of parameters.

Figure 3 illustrates stable time traces of the pulse intensity and the net gain per cavity round trip,  $G = g - q + \ln \kappa$ , for three different values of  $g_0$  on the  $P_1$  branch. Surprisingly, New's stability criterion is satisfied only in Fig. 3(b). This criterion stipulates that  $G < 0$  between pulses when  $|a|^2$  is small to prevent the growth of fluctuations on the wings of the pulses.<sup>2</sup> In other words, the zero intensity background has to be stable between pulses. However, Figs. 3(a) and 3(c) clearly contradict this point.

In Fig. 3(c) the net gain window is opened well before the arrival of a pulse in the course of the carrier density recovery process. This might be explained by analogy with the  $Q$ -switched dynamics of lasers with a saturable absorber.<sup>13</sup> In that context the phase space trajectory spends most of the time between the pulses near the so-called slow manifold corresponding to zero laser intensity, passing from its stable part to the unstable one. A pulse starts to develop only when the cumulative gain becomes positive, which means that the  $Q$ -switching pulse [similarly to the ML pulse shown in Fig. 3(c)] always has an unstable background at the leading edge.

More generally, stable ML pulses with an unstable background can exist because of the difference between pulse group velocity  $v_p$  and group velocity  $v_0$  of small perturbations. Consider a ML regime with period  $T_p = T + \delta T$ , with  $\delta T \ll T$ . The group velocity of the pulse is then  $v_p = vT/T_p \approx v(1 - \delta T/T)$ , where  $v$  is the group velocity in the cold cavity. On the other hand, for small perturbations, we note that for large enough  $\gamma T$ ,  $\dot{a}(t) + \gamma a(t) \approx \gamma a(t + \gamma^{-1})$ . Substituting

this relation into the left-hand side of Eq. (4), we conclude that the round-trip time for small perturbations is approximately  $T + \gamma^{-1}$ , which yields a velocity  $v_0 \approx v[1 - (\gamma T)^{-1}]$ . ML pulses with an unstable leading edge shown in Fig. 3(c) are stable because they move faster than the perturbation. Similarly, pulses with an unstable background on the trailing edge can be stable if they move slower than the perturbation, as for the parameter values of Fig. 3(a). The latter situation was already noted by Paschotta and Keller.<sup>14</sup>

To conclude, we have derived a DDE model for passive ML. Its extension to active or hybrid ML and inclusion of additional microscopic effects, e.g., carrier heating, is straightforward. This model is easy to simulate and analyze. It describes the appearance of ML pulses with an unstable background that are missing in the classical ML theories developed by New and Haus. Unlike the symmetric sech pulses of the Haus theory, the pulses with unstable background are asymmetric and can exist in the case of high cavity losses, i.e., in a situation typical of a semiconductor laser.

A. G. Vladimirov's e-mail address is vladimir@wias-berlin.de.

\*On leave from St. Petersburg State University, St. Petersburg 198904, Russia.

## References

1. P. Vasil'ev, *Ultrafast Diode Lasers: Fundamentals and Applications* (Artech House, Norwood, Mass., 1995).
2. G. H. C. New, *IEEE J. Quantum Electron.* **QE-10**, 115 (1974).
3. H. Haus, *IEEE J. Sel. Top. Quantum Electron.* **6**, 1173 (2000).
4. E. A. Avrutin, J. H. Marsh, and E. L. Portnoi, *IEE Proc. Optoelectron.* **147**, 251 (2000).
5. H. Haus, *IEEE J. Quantum Electron.* **QE-11**, 736 (1975).
6. H. Haus, *Jpn. J. Appl. Phys.* **20**, 1007 (1981).
7. H. A. Haus, C. V. Shank, and E. P. Ippen, *Opt. Commun.* **15**, 29 (1975).
8. J. C. Chen, H. A. Haus, and E. P. Ippen, *IEEE J. Quantum Electron.* **29**, 1228 (1993).
9. V. B. Khalfin, J. M. Arnold, and J. H. Marsh, *IEEE J. Sel. Top. Quantum Electron.* **1**, 523 (1995).
10. S. L. McCall and P. M. Platzman, *IEEE J. Quantum Electron.* **QE-21**, 1899 (1985).
11. K. Engelborghs, T. Luzyanina, and G. Samaey, "DDE-BIFTOOL v.2.00: a Matlab package for bifurcation analysis of delay differential equations," Tech. Rep. TW-330 (Department of Computer Science, Katholieke Universitet Leuven, Leuven, Belgium, 2001).
12. J. Palaski and K. Y. Lau, *Appl. Phys. Lett.* **59**, 7 (1991).
13. T. Erneux, *J. Opt. Soc. Am. B* **5**, 1063 (1988).
14. R. Paschotta and U. Keller, *Appl. Phys. B* **73**, 653 (2001).